DALTON PERSPECTIVE

Jahn–Teller effects in solid-state co-ordination chemistry

Larry R. Falvello

University of Zaragoza-C.S.I.C., Department of Inorganic Chemistry, Plaza San Francisco s/n, E-50009 Zaragoza, Spain

Jahn–Teller-active systems continue to yield unforeseen effects in the solid state. The use of conceptually simple potential energy surfaces, an approach developed by several investigators in recent decades, facilitates the understanding of diverse phenomena driven by Jahn–Teller activity. The background of this approach and its recent use in understanding dynamic Jahn–Teller systems, solid solutions of Jahn–Teller compounds in host lattices, and molecular shape switching in Jahn–Teller complexes are presented.

It has been sixty years since the well known theorem of Jahn and Teller was first expounded and proved. The interest inherent in it and the importance of its consequences are evident not only in the results of the ample number of studies of Jahn–Teller (JT) active systems carried out over the years, but also in the very fact that after six decades the theorem and derivative and related physical phenomena, often referred to by the global term 'Jahn–Teller effects', continue to be the subjects of active research.

Physical phenomena related to the Jahn–Teller theorem have been investigated not only in order to characterize JT effects themselves but also in order to use Jahn–Teller-active sites as probes into other physical systems.

In co-ordination chemistry the most commonly observed manifestation of the consequences of the Jahn–Teller theorem is a tetragonal distortion of octahedral complexes with degenerate electronic ground states. This distortion, normally by elongation of a pair of metal–ligand bonds, is more often than not characterized by diffraction analysis. However, in fact Jahn–Teller effects encompass a varied group of experimentally observable results; more importantly, they have been implicated in physical phenomena of importance in both basic and applied research. For example, Jahn–Teller effects have been proposed as an important factor in high-T_c cuprate superconductors,[1] and models have been put forward to describe the role of Jahn–Teller-active centers in these systems.[2–4] In a more directly promising development, Jahn–Teller effects have also been proposed as a critical factor in colossal magnetoresistance, a thousandfold increase in the magnitude of the magnetoresistance registered for normal magnetic media-reading devices such as magnetic tape and disk readers. Colossal magnetoresistance, which has been observed in systems containing the Jahn–Teller-active Mn^{3+} center,[5] has great potential for industrial applications in the rapidly expanding data storage media industry. Convincing evidence has been put forward that the Jahn–Teller effect at the manganese center is a causal factor for this phenomenon.[6,7]

This Perspective will present a critical overview of several areas of current study of Jahn–Teller effects in solid-state co-ordination chemistry. After an introduction to Jahn–Teller effects in general, including pseudo-JT and co-operative JT effects, recent research into dynamic JT phenomena in the solid state and studies of molecular solid solutions of Jahn–Teller active systems in non-JT hosts will be reviewed. The recently characterized phenomenon of 'Jahn–Teller switching' in solids will be described; this involves a concerted change of the direction of JT distortion within a single crystalline system in response to applied stress.

Jahn–Teller Effects in General

The theorem of Jahn and Teller[8] states that a non-linear molecule with a partially filled set of degenerate orbitals will be unstable with respect to distortion,[9,*] because there will exist at least one molecular distortion leading to a lowering of the energy of the molecule. The commonest manifestation of this theorem in co-ordination chemistry to date has been the often observed tetragonal elongation of a pair of mutually *trans* metal–ligand bonds in six-co-ordinate complexes of d^9 copper(II), or of high-spin d^4 chromium(II) or manganese(III), which have a single electron or hole in a set of e_g orbitals (Fig. 1). The degeneracy is removed by elongation of the two metal–ligand bonds in the z direction, giving rise to the orbital splittings of Fig. 1(*b*). The theory admits compression as a possibility on an equal footing with elongation.

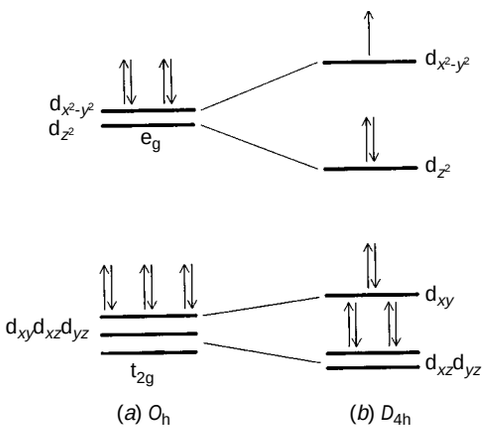

Fig. 1 Orbital splitting diagram for a complex with O_h symmetry, affected by Jahn–Teller elongation along the z axis

Jahn and Teller proved their theorem by a consideration of the energy of a symmetrical system and the perturbation energies arising from distortions from the symmetrical arrangement of the positions of the atomic nuclei. They showed that under conditions of orbital degeneracy the perturbation energies were negative for certain sets of atomic displacements, such as the movement of two ligands of an octahedral d^9 complex away from the central metal, and that thus the symmetrical arrangement of the atoms was unstable with respect to this distortion. The Jahn–Teller theorem was reformulated in terms of intramolecular forces by Clinton and Rice.[10] Their treatment, although mathematically rigorous, permits a simple statement of the origins of Jahn–Teller effects: if a molecule

* For the record, Jahn and Teller[8] stated and proved the following: 'all non-linear nuclear configurations are therefore unstable for an orbitally degenerate electronic state'. Jahn[9] stated the theorem thus: 'a configuration of a polyatomic molecule for an electronic state having orbital degeneracy cannot be stable with respect to all displacements of the nuclei unless in the original configuration the nuclei all lie on a straight line'.

with a proposed shape, for example a regular octahedral transition-metal complex, has a partially filled set of degenerate orbitals, for example the e_g set in a copper(II) complex, then the distribution of electron density necessarily possesses lower symmetry than does the distribution of atomic nuclei. This in turn necessarily gives rise to non-zero forces at some or all of the atomic nuclei, and thus the proposed molecule is unstable with respect to distortion. It is usually stated that the symmetrical molecule spontaneously undergoes a distortion, although the question of whether the symmetrical molecule exists for a significant amount of time in the first place requires a more rigorous analysis.

An important practical aspect of the Jahn–Teller theorem in co-ordination chemistry also arises naturally from a conceptualization based on the forces caused by an electron distribution with lower symmetry than the nuclear arrangement, namely that the Jahn–Teller effect is more pronounced for systems in which the degeneracy involves orbitals that significantly influence the metal–ligand bonding. Thus, important structural distortions are observed for octahedral transition-metal complexes with degenerate e orbital sets, such as Cu^{II}, high-spin Cr^{II}, and low-spin Co^{II}, but not for those with degenerate t sets, such as high-spin d^7 octahedral complexes of cobalt(II). This is because the σ-antibonding nature of the e set confers upon it more influence over the molecular shape than has the non-bonding or weakly π-bonding t set. Similarly, for tetrahedral complexes, in which the e orbital set is non-bonding and the t_2 set is antibonding, Jahn–Teller distortions can be expected for electron configurations with partial occupancy of the t_2 orbitals, d^3, d^4, d^8 and d^9.

This simple picture of Jahn–Teller effects and their origin is a useful guide in the routine activities of the co-ordination chemist. However, a more rigorous treatment is necessary for understanding many of the effects that arise in JT-active systems in the crystalline state. The original theorem and its consequences have been examined and reviewed in far more detail than that which they are usually accorded in co-ordination chemistry. A chronicle of the development of concepts related to Jahn–Teller effects has been given recently by Simmons.[11] Thorough reviews have been given by Hathaway,[12–14] Bersuker,[15] Hitchman[16] and others.

Jahn–Teller effects have a special niche in the phenomenology of chemistry, because they represent an exception to the Born–Oppenheimer approximation. That is, in a JT-active system, the distribution of electron density *does* influence the positions of the atomic nuclei in the molecule. In the case of a molecule for which the usual derivation of electronic wavefunctions for fixed nuclear positions would lead to a partially filled set of degenerate orbitals, the usual approximations used become invalid[17,18] and a rigorous solution of an *n*-fold degenerate system requires the use of *n* equations incorporating terms that mix the electronic and nuclear motions.[15] Such vibronic systems, with coupled electronic and nuclear structures, are fundamentally dynamic in nature. In the absence of external influences on its shape, a Jahn–Teller-active molecule would be fluxional, oscillating among *n* conformational energy minima of equal energy.

In practice, however, in a detailed examination of a Jahn–Teller active system, a rigorous solution of the wave equation is not derived. Rather, the adiabatic potential, that is the energy of the system derived from a Hamiltonian that does not include terms that mix the electronic and nuclear motions, is determined for a continuous set of molecular shapes including the symmetrical arrangement and also less symmetrical shapes that arise from distortions. A good deal of information can be obtained from such a description of potential energy as a function of molecular shape. The adiabatic potential can be represented conveniently by a surface or set of surfaces which represent potential energy as a function of 'distortion coordinates', in which the latter represent deviations from the symmetrical molecular shape that if maintained would give rise to electronic degeneracy.

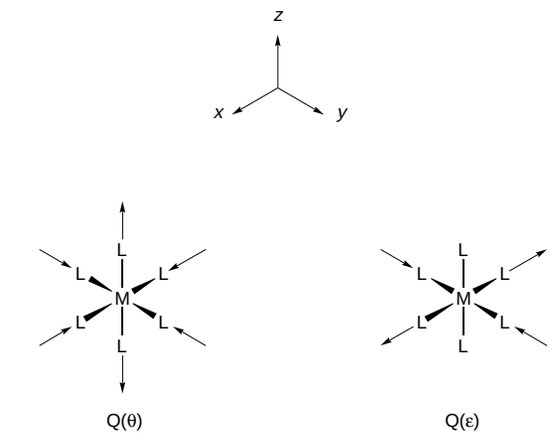

Fig. 2 The E_g distortions for an octahedral complex. More detailed descriptions of the Q(θ) and Q(ε) modes can be found in refs. 14, 15 or 19

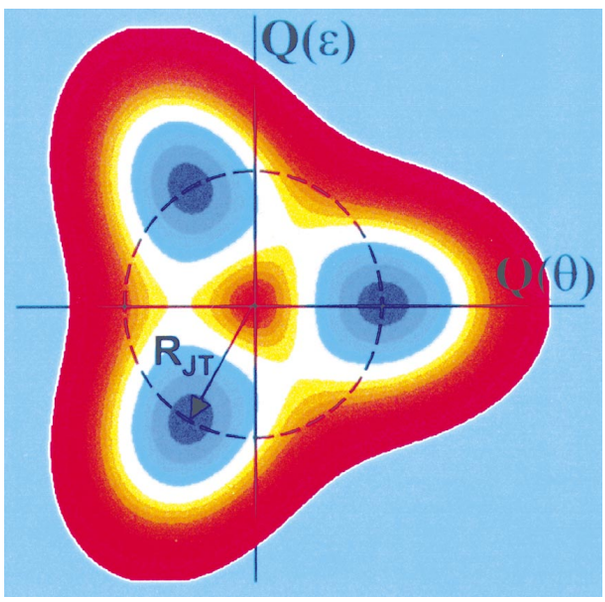

Fig. 3 Lower-energy adiabatic potential surface for a Jahn–Teller active octahedral complex. This surface has been called the 'warped Mexican hat potential energy surface'. Lower energies are represented by blue, higher by red

The Jahn–Teller system most often studied in co-ordination chemistry, namely an octahedral complex with a set of degenerate e_g orbitals possessing either a single electron or a single hole, serves as an example. A hypothetical complex with full O_h symmetry and an appropriate orbitally degenerate electron configuration (for example, d^9) is the conceptual point of departure. Most of the possible distortions of such a system are accompanied by restoring forces and give rise to vibrations. For such a molecule, though, there are two sets of nuclear motions which, according to the Jahn–Teller theorem, lead to a change of the total energy of the molecule and which do not have restoring forces that would lead to a return to O_h symmetry. These two motions are shown in Fig. 2; together they form a basis for the E_g representation of the point group O_h. It is these two motions that are coupled to the electron configuration of the system. The energy of the molecule as a function of the magnitude of these deformations (*i.e.* as a function of distortion coordinates) is represented in Fig. 3. The energy surface of Fig. 3 is derived from a perturbation treatment taken to second order; it is the lower of two surfaces described by theory. The high-energy point at the center of the drawing corresponds to

the O_h conformation. The three energy wells correspond to elongations along the molecular x, y and z axes, each of which reduces the molecular symmetry to D_{4h}. For such a homoleptic system, in the absence of external influences, the elongations parallel to x, y and z are all equally favored, and an isolated molecule would be fluxional as long as the energy crests between the wells were not so large as to impede interchange among the three distorted conformers with D_{4h} symmetry. The change of the shape and symmetry of the molecule in turn are accompanied by splitting of what would have been the E_g orbital set under O_h symmetry into non-degenerate levels.† The so-called adiabatic potential energy surface in Fig. 3 is commonly called the 'warped Mexican hat potential'. Its shape is specific to octahedral Jahn–Teller systems.

With reference to Fig. 3, the energy difference between the potential of the fully symmetrical O_h system at the center of the plot and the potential at the bottom of one of the wells is called the Jahn–Teller energy, E_{JT}. The radial distance from the center of the plot to one of the wells is commonly referred to as the Jahn–Teller radius, R_{JT}, and in practice can be used as an indication of the magnitude of a Jahn–Teller distortion.

Pseudo-Jahn–Teller effects

For a non-homoleptic transition-metal complex possessing an appropriate electronic structure, for example a d^9 complex *trans*-CuL_4X_2, in which L and X are different types of ligands, molecular distortion can still be observed, although the hypothetical octahedral complex would not have orbital degeneracy. This can arise if the departure from degeneracy is not severe; this phenomenon is referred to as the pseudo-Jahn–Teller (PJT) effect. The theoretical treatment of such a system is formally different from that of a JT complex; but for conformations away from the symmetrical shape, the adiabatic potentials for a PJT system form surfaces that are qualitatively similar to those for pure Jahn–Teller complexes.[15]

Jahn–Teller Co-operativity

As already described, Jahn–Teller effects are fundamentally dynamic in nature. In a hypothetical gaseous phase a Jahn–Teller-active molecule would be dynamic, oscillating between a number of energetically degenerate shapes. The only limitation on the populations of the various molecular shapes predicted by theory for a particular molecule arises from the energy barrier that must be crossed in passing from one shape to another.

In the crystalline state, however, co-operativity can and often does give rise to the selection of a single, statically distorted shape for each molecule. In the absence of co-operativity, JT-active systems in the solid would adopt random distortions and could even oscillate among the degenerate shapes in the crystal, an effect observable by diffraction in the form of large displacement (thermal) parameters for the affected atoms. If Jahn–Teller co-operativity is active, on the other hand, neighboring molecules in the crystal adopt aligned or otherwise related distortions, necessarily effecting a more compact packing arrangement and a decrease in the overall entropy of the crystal.

This co-operative Jahn–Teller effect has largely conditioned the conceptual view of Jahn–Teller systems in co-ordination chemistry. Since much of what is presently known about molecular shape has been established by X-ray crystallography, a technique which under routine interpretation gives a deceptively static view of its object, it is natural that the most commonly observed manifestation of the Jahn–Teller theorem has been a static distortion around certain transition-metal centers, as seen in lists of bond distances. The nature and practical implications of Jahn–Teller co-operativity, as well as its place as a special case of a more general phenomenon, have been understood from the beginning; in the pathmark works on the application of the Jahn–Teller theorem to inorganic chemistry, Orgel and Dunitz[20,21] invoked the theorem to explain the 'unusual', *i.e.* distorted, stereochemistry of copper(II) compounds as observed in crystal structures, and they described co-operative phenomena or 'trapping' as special crystalline-state manifestations of the usually dynamic Jahn–Teller effect.

The static, co-operative Jahn–Teller effects are best understood within the fuller context of the adiabatic potential surfaces described above. What is observed in a 'static' octahedral Jahn–Teller system in the solid, for example, is a molecule that is locked into one of the energy wells of Fig. 3, with two long and four short M–L bonds. The Jahn–Teller radius, R_{JT}, can be calculated from the metal–ligand bond distances of a distorted octahedral system by use of equation (1), in which

$$R_{JT}^2 = \sum_{i=1}^{6} \Delta d_i^2 \quad (1)$$

Δd_i represents the deviation of the ith M–L bond distance from the mean of the six.

Jahn–Teller co-operativity occurs when the magnitude of the perturbing forces caused by a crystalline environment is great enough to impede the full dynamic expression of the Jahn–Teller effect, but not large enough to suppress the distortion completely. In such a case, the crystalline environment is responsible for the qualitative fact that a single molecular distortion is observed; but the magnitude of the distortion is determined to a significant extent by the vibronic properties of the molecule and is at least partly independent of the surroundings. This 'vibronic amplification of distorting perturbations', which has been discussed in detail by Bersuker,[15] at first glance seems counterintuitive; but it derives support from the consistency in the values of R_{JT} derived from crystal structures of statically distorted Jahn–Teller complexes of a given transition element with similar ligand sets. This represents the static limit of the Jahn–Teller effect. At the opposite energetic extreme, under appropriate conditions of low energy barriers, weak crystal packing, or high temperature, the JT system can in principle course through the circular energy valley with radius R_{JT}, passing through any or all of the energy wells and saddle points. In other words, under the right conditions all three possible tetragonal distortions can exist at the same site in a crystal, interchanging dynamically.

An early example of Jahn–Teller co-operativity was observed in copper hexafluorosilicate, doped into the analogous zinc compound, $[Zn(H_2O)_6][SiF_6]$. At that time there was apparently no clearly established view of the consequences for co-ordination chemistry of the then recently expounded Jahn–Teller theorem. For the mixed Cu/Zn fluorosilicate, at temperatures as low as 90 K, the EPR spectrum was isotropic ($g = 2.24$),[22] whereas the EPR spectrum of a distorted copper center should be axial. A theoretical analysis did not agree with the observed data,[23] so it was concluded that the crystal field around copper in the solid must somehow represent an average of distorted molecular shapes. It was not possible to discern from the available data whether the isotropic g value represented a time or space average, that is whether the crystal was dynamically or statically disordered. Later measurement of the EPR spectrum of the doped fluorosilicate at temperatures below 60 K showed marked changes in the system; and at 20 K the spectrum had evolved to show the anisotropic picture expected for a distorted six-co-ordinate copper center with $g_\parallel = 2.46$ and $g_\perp = 2.11$.[24] This change was fully reversible with temperature. It was concluded from these experiments that the host lattice of $[Zn(H_2O)_6][SiF_6]$ permits a dynamic expression

† Although it is common to regard the removal of orbital degeneracy as a causal factor in Jahn–Teller effects, it is interesting that Jahn and Teller considered this an afterthought: '. . . there is the added complication that the nuclear displacements in question cause a splitting of the degenerate electronic state into states with different energies.'[8]

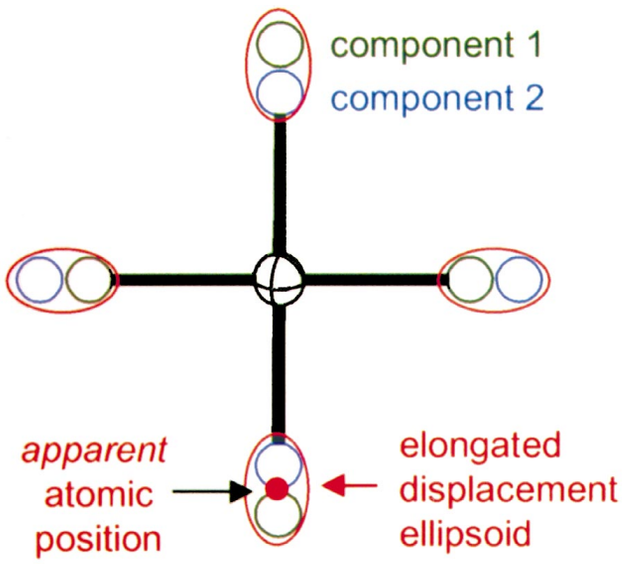

Fig. 4 Origin of the observed displacement parameters for an unresolved static disorder. Dynamic disorder gives a similar picture

of the Jahn–Teller effect of the guest copper centers at higher temperatures, but that ordering occurs at lower temperatures so that not only are the copper complexes trapped in a single tetragonally elongated shape, but these now-distorted molecules are aligned with each other throughout the crystal.

The simple qualitative concept of co-operativity is extensible to a more accurate and somewhat involved treatment of the strains produced in Jahn–Teller-active molecules by interactions with their surroundings in the solid state. The effects of such strain on the conformational energy surface for a given system can be characterized to a high level of detail, as discussed in analyses by Hitchman[16] and by Reinen and Atanasov.[25] Such treatments have been applied to the EPR spectra of CuF_6^{4-} in low concentration in K_2ZnF_4,[26] to that of Cu^{II} doped into various zinc Tutton salts,[27] and to those of $[Cu(H_2O)_2Cl_4]^{2-}$, $[Cu(NH_3)_2Cl_4]^{2-}$ and $[Cu(H_2O)(NH_3)Cl_4]^{2-}$, all in low concentrations in a host lattice.[28]

Dynamic Jahn–Teller effects

The term dynamic Jahn–Teller effects encompasses the growing body of observed solid-state systems in which a Jahn–Teller or pseudo-Jahn–Teller molecule is found in a crystalline surrounding elastic enough to permit fluxionality among the various minimum-energy shapes predicted by the Jahn–Teller theorem. For an octahedral copper complex, for example, this would mean that the complex is free to adopt any of the three tetragonal elongations predicted by theory, and to interchange among them continuously at a single site in the crystal. Several variations on this theme are possible: for example, a crystal might be sufficiently elastic to permit dynamic expression of two, but not all three, possible distortions.

The simplest case of a dynamic Jahn–Teller effect is an octahedral complex situated at a crystallographic site of cubic or trigonal symmetry in flexible surroundings. A recent example is a study of hexaaquacopper(II) bromate,[29] $[Cu(H_2O)_6][BrO_3]_2$, which will also serve to illustrate a method of characterizing such systems using X-ray diffraction. Based on the behavior of most six-co-ordinate copper complexes, it could reasonably be expected that the hexaaquacopper complex would display a substantial tetragonal distortion, with two Cu–O bonds, *trans* to each other, significantly elongated relative to the other four. However, in the bromate, the $[Cu(H_2O)_6]^{2+}$ moiety is located at a crystallographic site of symmetry $\bar{3}$ in the cubic space group $Pa\bar{3}$, and all six Cu–O distances are equivalent by symmetry, with a value of 2.079(4) Å. All O–Cu–O angles are essentially 90°, although this is not required by the crystallographic symmetry.

Despite the apparent symmetry of the system, as seen in the bond distances and angles, the X-ray diffraction analysis still reveals it to be Jahn–Teller active, through the anisotropic displacement parameters (thermal parameters). In the case of a dynamic disorder, or of a static disorder in which the atomic congeners are not well separated from each other, what is observed by diffraction methods is an average position of the atom in question, accompanied by an enlargement of the thermal parameters in the direction of the displacement generated by disorder. This is illustrated in Fig. 4, in which one plane of two disordered congeners of a hypothetical distorted complex are shown superposed. The X-ray diffraction experiment, which takes an average over the whole crystal and over time, yields a picture in which a single, average atomic site is observed for each of the affected atoms and in which the thermal parameters indicate the displacement caused by disorder.‡

A brief digression into the use of the commonly overlooked anisotropic displacement parameters will be useful before we proceed to a further interpretation of the structure of hexaaquacopper(II) bromate. In that structure the thermal parameters of the water oxygen atoms are larger than expected, as are the corresponding thermal ellipsoids. Anisotropic displacement parameters, which are almost always used for non-hydrogen atoms in routine structure analyses, are the elements of a 3 × 3 matrix from which one can derive an ample amount of useful information about the motion of an atom about its mean position in a crystal. When used together, moreover, the displacement parameters of groups of atoms in a crystal structure can yield more global information about the movement of chemically related groups in a structure. The simplest use of displacement parameters for a Jahn–Teller system is for determining whether a ligated atom, as for example a water oxygen atom in $[Cu(H_2O)_6]^{2+}$, shows considerably more displacement than does the metal atom to which it is attached. Such a difference is expected if a ligated atom is oscillating between having short and long bond distances to a Jahn–Teller-active metal center in a dynamic system. The displacement disparity, if present, can then be interpreted together with any other relevant data in order to determine whether a dynamic Jahn–Teller effect, or some other phenomenon, is operative.

The motion, or more precisely the mean-square displacement, of an atom in a given direction in a crystal is given by equation (2),[30]§ in which U_{ij}, with dimensions of $Å^2$, is the *ij*th

$$\mathrm{MSDA} = \left[\sum_{i=1}^{3}\sum_{j=1}^{3} U_{ij}\, n_i\, n_j\right] / |\boldsymbol{n}|^2 \qquad (2)$$

element (*i*th row, *j*th column) of the 3 × 3 matrix of thermal parameters. The quantities n_i, $i = 1$ to 3, are the elements of a vector in the direction under consideration, expressed in fractional crystallographic coordinates; MSDA is the desired mean-square displacement amplitude of the atom in the direction specified by vector *n*. One can calculate this quantity for any atom that has been refined anisotropically.

The difference between the MSDA of a ligated atom along a metal–ligand bond and the MSDA of the metal along the same bond is called ΔMSDA, or equivalently $\langle \Delta d^2 \rangle$, for that bond. That is, ΔMSDA for a metal–ligand bond is computed as MSDA(ligand) − MSDA(metal), with both MSDAs calculated

‡ The term 'displacement parameters' has been suggested as a replacement for 'thermal parameters' because the parameters in question are able to represent, as in the case described here, displacements caused by effects other than the temperature-dependent vibrations that they were first used to describe. In this Perspective the terms 'displacement parameters' and 'thermal parameters' are used interchangeably.

§ The program THMA 11[30] provides a convenient means of calculating ΔMSDA values from crystal structure results.

for the direction of the M–L bond. This ΔMSDA is the quantity that enters into comparisons with other like quantities for the purpose of determining whether disorder is present. Values of ΔMSDA are typically found in the range of (10–100) × 10^{-4} Å^2 and are commonly reported in units of 10^{-4} Å^2.

In the case of the hexaaquametal(II) bromates the ΔMSDA values (in 10^{-4} Å^2) for the complexes of Co, Ni and Cu, 48, 38 and 216 respectively,[29] show that the copper complex has nearly an order of magnitude disparity in the relative displacements of metal and ligand atoms, as compared to the analogous cobalt and nickel complexes. This was interpreted as signifying the presence of a dynamic Jahn–Teller effect in crystals of the copper complex, with the tacit conclusion that the augmented ligand displacements were caused principally by motion and not by static disorder.

It is also possible to quantify the Jahn–Teller distortion in terms of the JT radius in cases of dynamic disorder. Using the notation $\langle \Delta d^2 \rangle_{obs}$ for ΔMSDA, we can express the Jahn–Teller radius as in equation (3), in which the sum is taken over all

$$(R_{JT})^2 = \sum_{i=1}^{6} \langle \Delta d_i^2 \rangle_{obs} - \sum_{i=1}^{6} \langle \Delta d_i^2 \rangle_{res} \qquad (3)$$

metal–ligand bonds. The residual term $\langle \Delta d^2 \rangle_{res}$ represents that part of the relative motion of two atoms that is not brought on by the Jahn–Teller effect. This comparatively small term arises from all other M–L stretching modes and possibly non-systematic experimental error, least-squares correlation in the structure refinement, or other factors. In practice, the residual terms are estimated as the ΔMSDA values derived from the structures of chemically and if possible crystallographically analogous systems without Jahn–Teller active metals. For $[Cu(H_2O)_6][BrO_3]_2$ the ΔMSDA values from the structures of the nickel(II) and cobalt(II) analogues were used to estimate $\langle \Delta d^2 \rangle_{res}$ and a Jahn–Teller radius of 0.32(2) Å was calculated for the copper complex.

Similar behavior is shown by crystals of the chromium complex $[Cr(H_2O)_6][SiF_6]$, in which the hexaaquachromium sits on a site of $\bar{3}$ symmetry in space group $R\bar{3}$.[31] That system, with six crystallographically equivalent Cr–O bonds, was first interpreted as a case of Jahn–Teller suppression. Further examination of the anisotropic displacement parameters indicates that the Jahn–Teller effect is still manifest, with R_{JT} = 0.32 Å (uncorrected for $\langle \Delta d^2 \rangle_{res}$). Even so, an ambiguity remains, because a single X-ray diffraction experiment cannot in this case distinguish between static and dynamic disorder. So as far as the diffraction experiment can tell, the $[Cr(H_2O)_6]^{2+}$ may be dynamically disordered, oscillating at a given site among the three structures with elongation along each of the three mutually perpendicular M–L directions; or it may be statically disordered among the three elongated structures, with a single elongation present at a given site. Other considerations, such as the symmetry of the crystalline surroundings, lead to a conclusion that the JT effect must be dynamic; but experimental evidence is needed for a definitive result to be claimed. Under favorable conditions this sort of ambiguity can be resolved, in the simplest case with diffraction measurements at several temperatures. In the case of $[Cr(H_2O)_6][SiF_6]$, its acutely hygroscopic nature causes experimental difficulties; nevertheless, further studies are presently underway with the aim of characterizing the nature of its Jahn–Teller effect.

A comprehensive and detailed analysis of the means of characterizing both static and dynamic Jahn–Teller effects has been given by Bürgi and co-workers.[19] Their analysis has served as a conceptual point of departure for several recent studies. The object of the experimental part of their study was the cation $[Cu(tach)_2]^{2+}$, (tach = *cis*,*cis*-1,3,5-triaminocyclohexane) (Fig. 5) in which the two tridentate tach ligands form an octahedral environment about copper. The crystal structures of the perchlorate and the nitrate were done at room temperature, and powder EPR spectra were measured for both salts at temperatures from 4 to 300 K. In addition, single-crystal EPR spectra were measured at room temperature for the perchlorate and from 4 to 300 K for the nitrate.

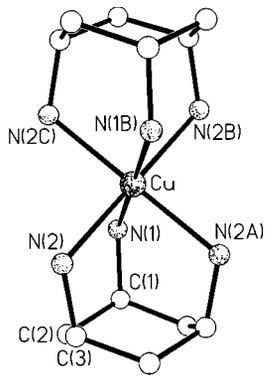

Fig. 5 Drawing of $[Cu(tach)_2]^{2+}$. Atomic coordinates, from the crystal structure of the nitrate, were extracted from the Cambridge Crystallographic Database

The perchlorate salt was found to display static Jahn–Teller distortion in the temperature range of 4–300 K, as seen at room temperature in the crystal structure and at all temperatures in anisotropy of the EPR spectrum. At 4 K the effective *g* values are 2.203(4), 2.100(10) and 2.061(4), typical of the values found for a static tetragonal elongation. In the room-temperature single-crystal EPR spectrum the effective *g* values are only slightly less anisotropic, 2.190(3), 2.106(3) and 2.086(3). The nitrate salt, on the other hand, was observed to have static distortion only in the range 4–120 K, for which *g* values of 2.250(2), 2.081(2) and 2.047(2) were seen. Above 120 K the EPR experiment revealed a dynamic Jahn–Teller effect in which the complex oscillates between two of the three possible tetragonal elongations. For example, just above 120 K the *g* values are 2.171(4), 2.154(3) and 2.068(3), of which the two higher figures are time averages of high and low *g* values, indicating that two of the metal–ligand bond directions are oscillating between long and short variants.¶ This type of Jahn–Teller expression has been called a 'static dynamic' or 'planar dynamic' Jahn–Teller effect.[32] The spectrum gradually loses all anisotropy until at 230 K the *g* values are 2.143(5), 2.142(4) and 2.111(4), suffering only slight changes at still higher temperatures. The isotropy of the spectrum at higher temperatures is most easily explained by a fully dynamic Jahn–Teller effect, with all metal–ligand bonds in a given molecule oscillating in a concerted fashion between short and long distortions. These results, in addition to establishing the nature of the Jahn–Teller effects in the perchlorate and nitrate salts, demonstrate the usefulness of EPR spectra in analysing JT effects.

It was possible to correlate the EPR results for the two salts of $[Cu(tach)_2]^{2+}$ with the crystal structures determined at room temperature. For the ClO_4^- salt the X-ray analysis showed a static distortion, with unique Cu–N bond distances of 2.353(7), 2.061(6) and 2.078(6) Å; from these values a Jahn–Teller radius of 0.328 Å is calculated. In the nitrate salt the copper atom sits on a site of 2/*m* symmetry, with two of the six M–L bond distances, related to each other by symmetry, having a common value of 2.173(6) Å, and with the other four, also symmetry related to each other, having a value of 2.164(3) Å. Despite the apparent equivalence of the bond distances about the metal, the anisotropic displacement parameters reveal the Jahn–Teller

¶ As expounded by Bürgi and co-workers, the EPR spectrum above 120 K could in principle also be explained by magnetic exchange coupling between statically distorted complexes at different crystallographic sites. All other evidence from this and other systems points to an interpretation based on the static dynamic Jahn–Teller expression.

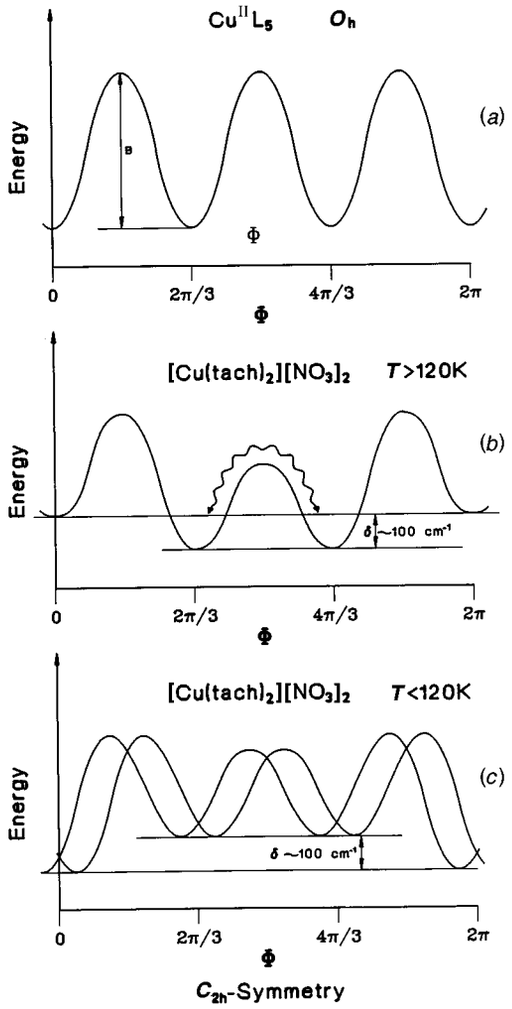

Fig. 6 Circular section through the adiabatic potential energy surface of a Jahn–Teller active system, taken at a radius of R_{JT}.[19] Reproduced with permission from the American Chemical Society

effect. The Jahn–Teller radius calculated from equation (3) and using displacement parameters from the structure of the analogous nickel compound to estimate $\langle d_i^2 \rangle_{res}$, is 0.329 Å, in good agreement with the value calculated for the statically distorted ClO_4^- salt. (An R_{JT} value of 0.320 Å was derived separately for the nitrate salt from an analysis of thermal parameters based on group motion.) The values of R_{JT} derived for the two salts of $[Cu(tach)_2]^{2+}$ were compared to those of ten other homoleptic copper(II) complexes that had been reported previously, and whose values of R_{JT} vary within the range of 0.252 to 0.358 Å. The average value of 0.320 Å for the group of 12 complexes had a standard deviation of 0.029 Å, which shows the remarkable consistency of Jahn–Teller radii among these CuN_6 chromophores in varied crystalline environments.

Bürgi *et al.*[19] used the EPR data to derive information about the 'angular potential parameters' for the copper complexes. This term refers to parameters describing the shape of a circular cross-section through the adiabatic potential energy surface of Fig. 3. Laid out in a plane, this section, taken at a radius of R_{JT} has the idealized appearance shown in Fig. 6(*a*). In the gas phase in the absence of external perturbations the energy curve has three minima corresponding to the three tetragonally elongated molecular distortions. The barriers of energy B between minima are passable if sufficient thermal energy is present. In the solid the minima may or may not have the same energy; one or two minima may have higher energy than the other(s), as a result of constraints imposed by the surroundings of the molecule; or all three could be of different energies. From the EPR data for $[Cu(tach)_2][NO_3]_2$ it was deduced that at temperatures below 120 K the angular potential has the shape

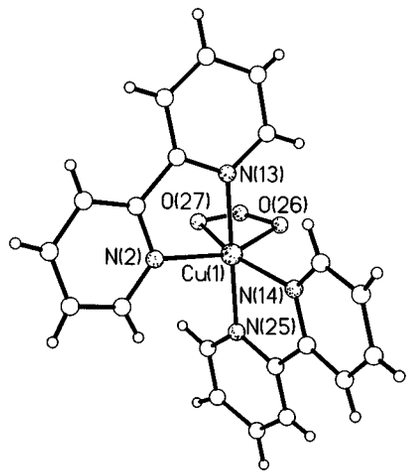

Fig. 7 One cation of $[Cu(bpy)_2(ONO)]^+$. Atomic coordinates are taken from the room-temperature structure determination of the nitrate, and were extracted from the Cambridge Crystallographic Database

shown in Fig. 6(*c*), with one tetragonal elongation lying in a potential well at about 100 cm^{-1} below the other two ($kT = 83.4$ cm^{-1} at 120 K). Thus the distortion is static and gives rise to the uniaxial g values observed at low temperature. At just above 120 K the angular potential has the shape shown in Fig. 6(*b*), with two elongated structures about 100 cm^{-1} lower in energy than the third. The barrier between the two lower-energy structures is passable, and in the crystal the complex oscillates between two elongated structures, giving two roughly equal, larger g values [2.171(4) and 2.154(3)] corresponding to the average of long and short Cu–N bonds for the two dynamic metal–ligand directions, and one lower g value of 2.068(3) for the static *trans* pair of short Cu–N bonds. As the temperature is increased further, thermal energy 'loosens' the crystalline surroundings even more, to the extent that at room temperature the angular potential has a shape with three accessible minima related by passable barriers; this gives a fully dynamic expression of the Jahn–Teller effect in the solid.

The experimental results for $[Cu(tach)_2][NO_3]_2$ and $[Cu(tach)_2][ClO_4]_2$, along with their interpretations, demonstrate that the Jahn–Teller effect is capable of giving results, such as time- and space-averaged bond distances from X-ray diffraction or time-averaged g values from EPR spectroscopy, that are deceptive when taken literally; but they also demonstrate that the same techniques can be used to extract not only the correct interpretations of the systems under study but even more detailed information than one expects to extract from a routine analysis. This fact has been particularly well borne out in a study of the dynamic pseudo-Jahn–Teller system $[Cu(bpy)_2(ONO)][NO_3]$ (bpy = 2,2′-bipyridine) in which it was demonstrated that X-ray diffraction, theretofore widely considered to be confined to studies of single- or steady-state solids, could in fact be used to determine the energy differences between different molecular conformations.

That this is indeed possible was reported with full experimental details by Simmons *et al.*,[33] following their earlier exposition of the concept.[34–36] One $[Cu(bpy)_2(ONO)]^+$ cation is shown in Fig. 7, with the important ligated atoms labelled according to the naming scheme employed by the original authors. The point symmetry of the chromophore is C_2, and this is not formally a Jahn–Teller system. Its pseudo-Jahn–Teller nature derives from its relationship to a D_3 chromophore, such as $[Cu(bpy)_3]^{2+}$, which has a partially occupied ^2E ground state and is a JT system. Replacing one bpy ligand with nitrite changes the symmetry to C_2 and splits the ^2E state into ^2A and ^2B, with the former as the ground state. Although this is not now a Jahn–Teller-active system, the point group C_2 permits non-zero coupling of the ^2A and ^2B states, provided their energy

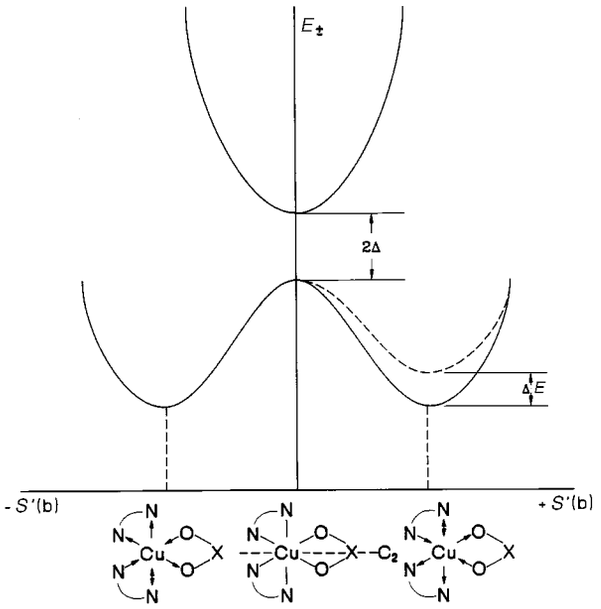

Fig. 8 Conformational energy curve for $[Cu(bpy)_2(ONO)]^+$.[33] Reproduced with permission from the American Chemical Society

difference is small, *via* a vibration of symmetry B; that is, a distortion that is antisymmetrical with respect to the two-fold axis lowers the energy of the system in a manner analogous to the way that a tetragonal elongation lowers the energy of an octahedral copper(II) complex. In other words, if the splitting of the A and B electronic states is not great, a molecule such as this will behave as a Jahn–Teller system and adopt distorted conformations in which, among other things, one of the *cis*-Cu–O bonds is longer than the other. The energy curve for such a distortion coordinate is shown in Fig. 8, in which the energy maximum at the center of the trace corresponds to an undistorted shape with C_2 symmetry and the two energy minima correspond to the distortions shown at the bottom of the figure.

Qualitatively, an X-ray diffraction analysis of such a system can show any of several major characteristics. If the crystalline surroundings are rigid and the system adopts a fully co-operative, static Jahn–Teller distortion one simply observes the fully distorted structure with one Cu–O bond significantly longer than the other, Cu(1)–O(26) ≈ 2.0 and Cu(1)–O(27) ≈ 2.5 Å. This corresponds to full population of one of the two energy minima in Fig. 8. At the other extreme, if the crystal packing is sufficiently elastic the molecule will be fully dynamic, oscillating between the two distorted conformations so that the bonds Cu(1)–O(26) and Cu(1)–O(27) exchange continuously between the long and short values. This corresponds to equal population of both energy wells of Fig. 8, and in a crystal structure one would see an average value in the vicinity of 2.2 Å for both Cu(1)–O(26) and Cu(1)–O(27). However, in this case one would also observe significantly augmented displacement parameters for both of the ligated oxygen atoms, with thermal ellipsoids elongated in a direction roughly parallel to the metal–ligand bond. In intermediate situations, in which the crystalline surroundings are unsymmetrical to the extent that they slightly favor one distorted conformation over the other but not to the extreme of a full static distortion, one would observe the effects of unequal non-zero populations of both energy minima. This case is illustrated in the potential energy diagram in Fig. 8, with the dotted line in the trough at the right representing a slight increase in the energy of one of the distorted structures, brought on by interactions with the crystalline environment. Now the populations of the two distorted structures can be expected to obey a Boltzmann distribution, and in a crystal structure determination an averaged partial distortion would be observed. The apparent Cu–O bond distances would be unequal, but less so than in the static limit, and the displacement ellipsoids would be elongated, but not as much as in the case of dynamic disorder between two equally populated structures.

In their report Simmons *et al.*[33] used the temperature variation of the relative populations of distortions with unequal energy as the means of determining the energy difference between the two distorted conformations in the solid. A formula was presented, based on the Boltzmann distribution, in which crystallographic observables were related to the temperature and to the energy difference between the two minima of Fig. 8. In the formula, given in equation (4), S' is the distortion

$$\Delta E = RT \ln [(S_{PJT} + S')/(S_{PJT} - S')] \quad (4)$$

coordinate at a given temperature T, R is the molar gas constant, and ΔE is the energy difference between the two distorted shapes of the cation, or more exactly between the lowest-energy vibronic levels of the two distorted structures. The quantity S' is the distortion coordinate, calculated from equation (5), in

$$S'^2 = \tfrac{1}{2}\{[\Delta d(Cu{-}O_{eq})]^2 + [\Delta d(Cu{-}N_{eq})]^2 + [\Delta d(Cu{-}N_{ax})]^2\} \quad (5)$$

which Δd represents the difference in apparent copper–ligand bond distances for the two (equatorial) oxygen atoms (O_{eq}), the two equatorial nitrogen atoms (N_{eq}), and for the axial nitrogen atoms (N_{ax}). The quantity S_{PJT} in equation (4) is the value of the distortion coordinate at the static limit; this was estimated from a structure determination at 20 K. The formula was based on the assumption that no vibronic levels other than those shown in Fig. 8 were significantly populated; a more rigorous formula was also presented for use in the event of a breakdown of that assumption.

X-Ray data taken at 20, 100, 165 and 296 K yielded the appropriate Δd values for use in equation (5) to calculate the distortion coordinate S' at each of these temperatures, and then a plot of $\ln[(S_{PJT} + S')/(S_{PJT} - S')]$ against T^{-1} yielded a value of 77 cm^{-1} for ΔE. This value is of the same order of magnitude as that obtained from EPR data for the energy difference between troughs for $[Cu(tach)_2][NO_3]_2$.[19]

This thermodynamic result is unusual, perhaps unprecedented, in having been derived entirely from single-crystal X-ray diffraction data. It is a good example of how developments in theory and experimental practice have accompanied the study of Jahn–Teller effects. In this regard, studies of dynamic JT effects have been especially fruitful in leading to more advanced use of single-crystal diffraction.

Molecular Solid Solutions of Jahn–Teller-active Compounds in Non-Jahn–Teller Hosts

Jahn–Teller systems have been examined in solid solution since the earliest studies of JT effects in co-ordination chemistry. One of the first experimental works on Jahn–Teller-active co-ordination compounds was the EPR study on copper-doped $[Zn(H_2O)_6][SiF_6]$ described above. A good number of solid solutions of JT-active systems in extended, non-molecular structures, oxides or halides, have been examined using primarily powder diffraction for characterizing their structures.

In recent years systematic experimental studies have appeared in which the responses of Jahn–Teller systems to incorporation in non-JT-active hosts have been examined in single crystals of molecular solids. In molecular solids the principal structural moieties, molecules or ions, are related by relatively weak forces, as opposed to the situation in extended oxide structures, for example, in which strong forces extend throughout the structure without any weak-interaction buffers

Table 1 Observed and apparent bond distances about the metal site for the *trans*-$[Cr_xZn_{1-x}(sac)_2(H_2O)_4]\cdot 2H_2O$ solid solutions

x(Cr)	M–N/Å	M–O(1w)/Å	M–O(2w)/Å
0.0	2.204(2)	2.061(2)	2.162(2)
0.382(9)	2.196(2)	2.055(2)	2.224(3)
0.493(8)	2.197(2)	2.057(2)	2.239(2)
0.56(2)	2.200(4)	2.056(4)	2.255(6)
0.63(1)	2.201(2)	2.056(2)	2.268(3)
0.69(1)	2.199(2)	2.054(2)	2.288(3)
1.00	2.197(2)	2.048(2)	2.399(3)

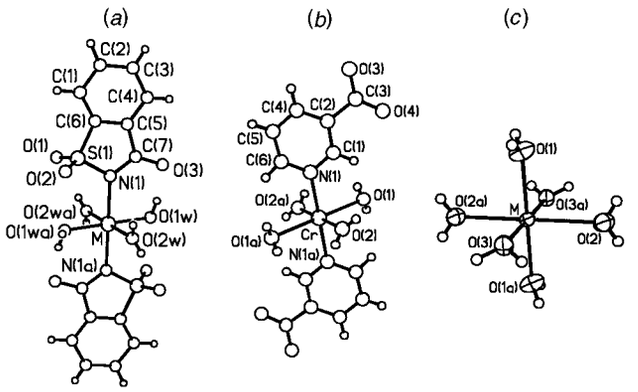

Fig. 9 Molecular drawings and atom naming schemes for (*a*) *trans*-[Cr/Zn$(sac)_2(H_2O)_4$], (*b*) *trans*-[Cr/Zn$(nic)_2(H_2O)_4$], and (*c*) [Cr/Zn$(H_2O)_6]^{2+}$ in the Tutton salt

between them. Thus, it could be expected that co-operativity effects will be expressed differently in molecular solids. The use of single crystals rather than powders for the study of molecular solid solutions was meant to assure to the extent possible the homogeneity of the samples and to provide a high level of accuracy in the structural results.

In three studies of solid solutions of Jahn–Teller active chromium complexes in non-Jahn–Teller zinc-containing hosts reported in the last decade three distinct responses to solid-solution formation have been observed for the JT-active molecules. The molecules in question are all six-co-ordinate chromium complexes in which the high-spin d^4 center, with one unpaired electron in the e_g orbital set, is subject to Jahn–Teller distortion.

The first complex, *trans*-$[Cr(sac)_2(H_2O)_4]$ (sac = saccharinate, $C_7H_4NO_3S^-$), Fig. 9(*a*), crystallizes as the dihydrate. The pure chromium complex, which is formally a pseudo-Jahn–Teller system, is isomorphous with the zinc complex.[37] Both crystallize in the monoclinic system, space group $P2_1/c$. (The JT-active copper complex also has the same crystal structure.[38,39]) For the chromium compound, the Jahn–Teller effect is seen in the crystal structure in the form of an elongation of the Cr–O(2w) bond [2.399(3) Å] relative to Cr–O(1w) [2.048(2) Å]; Cr–N(1) has the intermediate length 2.197(2) Å. For the pure chromium complex, $R_{JT} = 0.352$ Å.

Five molecular solid solutions of the chromium complex in the analogous zinc system, with the mole fraction of chromium, x(Cr), ranging from 0.382(9) to 0.69(1), were characterized by single-crystal X-ray diffraction at room temperature.[40] The M–L distances derived from these analyses are shown in Table 1. The most notable feature of the data in the table is the strong dependence of the M–O(2w) distance on composition, with values varying from pure-Cr value of 2.399(3) Å to 2.288(3) Å for x(Cr) = 0.69, then diminishing monotonically through the series to a value of 2.224(3) Å for x(Cr) = 0.382. In contrast, the M–N(1) bond length is constant through the entire series, and the second metal-to-water-oxygen distance, M–O(1w), shows a constant value throughout the solid solutions; this value is slightly longer than Cr–O(1w) for the pure chromium system and slightly shorter than the value in the pure zinc compound.

This set of geometrical features is consistent with the presence of disorder in the direction of the M–O(2w) bond, with O(2w) disordered over two sites, one closer to the metal for the zinc-containing positions and one farther from the metal for chromium. The two congeneric O(2w) sites are not far enough apart to be distinguished by X-ray diffraction at room temperature, and thus what emerges from the structure analysis is an average position. The M–O(2w) distances for the solid solutions would be 'apparent' distances, as discussed by Stebler and Bürgi;[41] they represent intermediate values between the shorter Zn–O(2w) and longer Cr–O(2w) distances, and are weighted by population. Thus, the apparent M–O(2w) distance increases with x(Cr).

If the conclusion of disorder in these solid solutions is correct, then the response of the chromium system to its incorporation into the non-Jahn–Teller host is essentially negligible. The JT system maintains its distortion, and the overall result is disorder of the atom affected by JT distortion, namely O(2w). Apparently, the intermolecular forces present in the form of an extensive hydrogen-bonding network are sufficiently strong to maintain Jahn–Teller co-operativity and the concomitant static distortion of the chromium complex, but are not sufficiently constraining so as to provoke a further response from the Jahn–Teller center.

The situation is quite different for the second system studied in molecular solid solutions, *trans*-$[Cr_xZn_{1-x}(nic)_2(H_2O)_4]$ (nic = nicotinate, $C_6H_4NO_2^-$), Fig. 9(*b*). In this case, the pure chromium and pure zinc complexes are not isomorphous in the crystalline state.[42] Crystals of the JT-distorted chromium complex are triclinic, space group $P\bar{1}$, and the chromium atom sits on a center of symmetry with one pair of Cr–O (water) bonds significantly elongated with respect to the other [Cr–O(1) 2.471(1), Cr–O(2) 2.047(1) and Cr–N(1) 2.129(1) Å; $R_{JT} = 0.450$ Å] in a pattern typical of pseudo-Jahn–Teller complexes. The zinc complex, on the other hand, crystallizes in the monoclinic space group $C2/m$ with the zinc atom residing on a site of symmetry $2/m$ and with all four Zn–O bonds equivalent by crystallographic symmetry. A two-fold axis bisects one opposing pair of O–Zn–O angles, and a crystallographic mirror bisects the other pair. Despite the significant differences between the two structures, it was demonstrated by Broderick, *et al.*[42] that solid solutions of the complexes of Cr and Zn could be formed. One solid solution had been characterized earlier.[43]

The response of these structurally different systems to the formation of solid solutions was not easily predictable. The type of result seen in the saccharinates, disorder between the zinc complex and a statically distorted chromium molecule, is not possible in this case if the monoclinic structure of the zinc complex is maintained, because the fully distorted chromium complex does not fit into the monoclinic structure. Simple modelling calculations showed that the distorted chromium complex, inserted into the monoclinic structure, forms implausible short contacts with its surroundings, whether they consist of the undistorted zinc compound or the distorted chromium complex.

In the actual event, it was found that up to a population of about 75% chromium the solid solutions adopted the monoclinic structure of the pure zinc compound, with all four M–O (water) distances equivalent by crystallographic symmetry.[44] Eight solid solutions with x(Cr) varying from 0.145(12) to 0.777(12) were examined using single-crystal X-ray diffraction. The bond distances about the composite Cr/Zn site are given in Table 2. The observed M–N distances change insignificantly as a function of composition, while the M–O distances suffer only a slight augmentation with increasing values of x(Cr). The bond distances do not show, and because of crystallographic symmetry cannot show, the effects of Jahn–Teller distortion of the chromium center. The slight changes in the M–O bond

Table 2 Observed bond distances about the metal site for the solid solutions *trans*-$[Cr_xZn_{1-x}(nic)_2(H_2O)_4]$. For $x(Cr) = 1.0$ the structure is triclinic, for all others monoclinic with all four M–O distances equivalent

x(Cr)	M–O/Å	M–N/Å	ΔMSDA/Å^2 × 10^4
0.0	2.122(1)	2.150(1)	29
0.145(12)	2.124(1)	2.154(2)	50
0.328(9)	2.138(1)	2.148(1)	107
0.397(9)	2.141(1)	2.148(1)	136
0.486(7)	2.148(1)	2.142(1)	157
0.539(10)	2.144(1)	2.148(2)	172
0.637(9)	2.159(1)	2.147(1)	216
0.749(9)	2.171(1)	2.147(1)	259
0.777(12)	2.168(2)	2.151(2)	254
1.0	2.475(1)	2.129(1)	89
	2.0473(9)		21

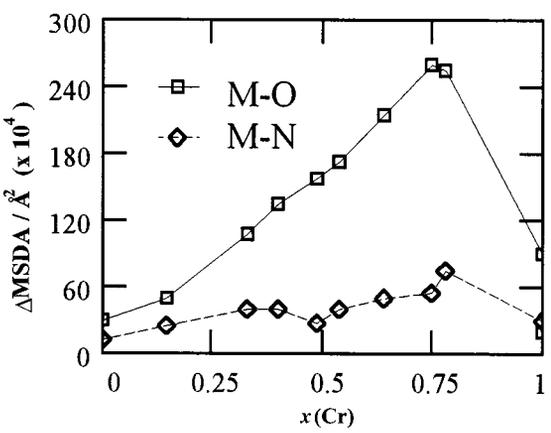

Fig. 10 Values of ΔMSDA (Å^2 × 10^{-4}) for the Cr/Zn–O and Cr/Zn–N bonds in the series of solid solutions *trans*-$[Cr_xZn_{1-x}(nic)_2(H_2O)_4]$

length across the series of solid solutions is accompanied by a similarly slight and practically isotropic increase in the unit-cell dimensions.

The expression of the Jahn–Teller effect is visible, however, in the anisotropic displacement parameters derived from the diffraction studies. The values of ΔMSDA [see equation (2) and the associated discussion] for the M–O bond increase monotonically across the series of solid solutions, as seen in Fig. 10. A detailed analysis of the anisotropic displacement parameters in this case is complicated by the fact that it is only possible to refine a single set of U_{ij} for the mixed metal and water oxygen sites, while it is probable that the displacement parameters for the individual zinc and chromium centers, as well as for the oxygen atoms bonded to them, are distinct. Thus, while it is clear from Fig. 10 that the Jahn–Teller effect is still expressed for the chromium center, a concrete conclusion regarding its nature cannot be derived from the presently available data. (The data on the Cr/Zn nicotinate solid solutions were taken mostly at room temperature. These data, along with recent variable-temperature diffraction results, are currently being re-examined.) Two quite different interpretations are possible. Firstly, it may be that the constraining crystalline environment of the solid solution limits the static pseudo-Jahn–Teller effect to a lesser distortion than that seen in the pure chromium complex, and that the two possible distortions are disordered over the two unique M–O directions. The second possibility is that the chromium center has switched to a dynamic Jahn–Teller effect, with vibronic displacements of limited amplitude. Given that either a static or a dynamic expression would likely be of restricted amplitude, dynamic disorder seems a more plausible explanation. A limited static expression would leave the molecule at a point on the adiabatic potential surface that did not correspond to an energy minimum, and which would not be far from a maximum; the potential energy surface would have to be oddly shaped to permit only such a partial scaling of the barrier between the two minimum-energy distortions without allowing a fully dynamic expression of the Jahn–Teller effect.

Whatever the final interpretation of the nicotinate solid solutions turns out to be, it is clear that the response of the chromium center to the constraints of the crystal structure is different from that displayed in the saccharinate solid solutions. While the saccharinate maintains a single direction of JT distortion in the solid solutions, the nicotinate necessarily has the Jahn–Teller expression spread over both directions in the e_g plane when cocrystallized with the zinc complex. In the unlikely event that the distortion is static for the chromium centers, the static distortion would be disordered over two M–L bond directions.

Still different behavior is displayed by solid solutions of the ammonium chromium Tutton salt, $[NH_4]_2[Cr(H_2O)_6][SO_4]_2$, in the analogous zinc compound. The copper and chromium Tutton salts, it should be noted, have been investigated in depth in connection with the Jahn–Teller effect (see Hathaway[14] and refs. therein), and their characterization has been augmented by accurate and detailed experimental charge-density[45] and thermal motion studies[46] along with theoretical calculations.[47]

Unlike the saccharinate and nicotinate complexes of chromium, the Tutton salt contains a pure, as opposed to pseudo, Jahn–Teller center. The hexaaquachromium(II) ion is in principle capable of adopting any of three distorted shapes, corresponding to the three energy wells in the 'warped Mexican hat' potential surface of Fig. 3. In crystals of the pure chromium salt at room temperature a co-operative Jahn–Teller effect is observed, with elongation of the M–O(2) bond and its inversion relative, M–O(2a), as shown in Table 3. The bond distances and displacement parameters appear to indicate the presence of some degree of dynamic behavior, however. The distances describe a rhombically rather than tetragonally distorted chromium center, with Cr–O(1) 2.121(1), Cr–O(2) 2.324(2) and Cr–O(3) 2.050(1) Å. So while Cr–O(2) suffers the principal elongation, Cr–O(1) also has an indication of distortion. That the Jahn–Teller effect is responsible for this can be tested by examination of ΔMSDA values derived from the anisotropic thermal parameters; their values in units of 10^{-4} Å^2 are 137 for Cr–O(1), 181 for Cr–O(2) and 37 for Cr–O(3). Thus, both O(1) and O(2) are disordered to some degree, although O(1) predominantly populates its site nearer the metal and O(2) a site farther away. The distances given for both O(1) and O(2) in Table 3 are then apparent, population-weighted average values. The aqua ligand at O(3) does not suffer disorder, and molecular conformations with elongated Cr–O(3) bonds are not present in the crystal. A variable-temperature structural and EPR study of the analogous copper Tutton salt showed that it was fluxional in the solid, with increasing population of one Cu–O elongation as the temperature decreased.[48] The behavior of the chromium system is consistent with that of its copper-containing analogue.

The ammonium Tutton salts of all of the first-series transition elements are practically isostructural, and the chromium- and zinc-containing salts form solid solutions across the full range of concentration. As in the cases of the nicotinates and saccharinates, intermolecular space in the Tutton salts is extensively bridged by hydrogen bonds. Solid solutions of the mixed Tutton salt $[NH_4]_2[Cr_xZn_{1-x}(H_2O)_6][SO_4]_2$ were examined by single-crystal diffraction at room temperature for seven different compositions ranging from $x(Cr) = 0.07(1)$ to 0.93(2).[49] Several features of the results stand out in contrast to what was observed for the saccharinate and nicotinate systems. First of all, in the Tutton salt solid solutions the apparent bond distances give the appearance of Jahn–Teller compression. A plot of bond distances *vs.* composition is shown in Fig. 11, from

Table 3 Observed and apparent metal–ligand bond distances and ΔMSDA values for $[Cr_xZn_{1-x}(H_2O)_6]^{2+}$ in the Tutton salts and their solid solutions, measured at room temperature by X-ray diffraction and at 11–16 K by neutron diffraction

	M–O(1)		M–O(2)		M–O(3)	
x(Cr)	Distance/Å	ΔMSDA/Å^2 × 10^{-4}	Distance/Å	ΔMSDA/Å^2 × 10^{-4}	Distance/Å	ΔMSDA/Å^2 × 10^{-4}
Room temperature, X-ray diffraction						
0.0	2.111(2)	22	2.104(3)	65	2.065(2)	3
0.07(1)	2.114(1)	42	2.108(1)	20	2.059(1)	30
0.10(1)	2.118(1)	53	2.110(1)	23	2.059(1)	17
0.22(1)	2.1312(1)	82	2.1143(1)	42	2.0568(1)	22
0.27(1)	2.138(1)	113	2.117(1)	53	2.058(1)	27
0.48(1)	2.161(2)	171	2.127(1)	99	2.056(1)	37
0.48(1)	2.164(1)	169	2.130(1)	95	2.057(1)	36
0.62(1)	2.184(2)	219	2.139(2)	143	2.055(2)	47
0.67(1)	2.188(2)	212	2.145(2)	148	2.054(1)	50
0.66(1)	2.191(2)	228	2.141(2)	152	2.057(1)	39
0.76(1)	2.199(1)	240	2.153(1)	164	2.053(1)	36
0.93(1)	2.207(4)	280	2.179(4)	243	2.048(3)	24
1.0	2.121(1)	137	2.324(2)	181	2.050(1)	37
11–16 K, neutron diffraction						
0.10	2.129(2)	70	2.103(2)	12	2.066(2)	14
0.22	2.133(2)	127	2.085(2)	11	2.053(2)	15

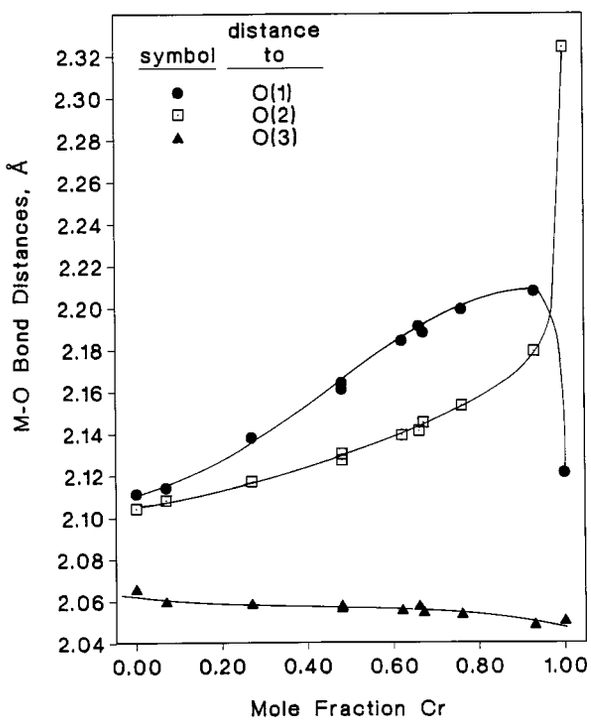

Fig. 11 Apparent M–O bond distances in the pure and mixed Tutton salts $[NH_4]_2[Cr_xZn_{1-x}(H_2O)_6][SO_4]_2$.[49] Reproduced with permission from the American Chemical Society

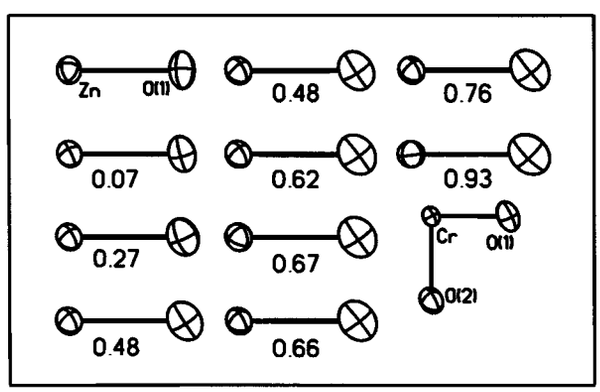

Fig. 12 Displacement ellipsoid montage for the M–O(1) bond across the series of solid solutions $[NH_4]_2[Cr_xZn_{1-x}(H_2O)_6][SO_4]_2$.[49] Reproduced with permission from the American Chemical Society

which it is seen that the apparent M–O(1) and M–O(2) distances are similar to each other in each of the solid solutions and that their apparent value decreases with decreasing x(Cr). In all of the mixed Cr/Zn crystals, the similar distances observed for M–O(1) and M–O(2) are significantly longer than M–O(3), which has a relatively constant value through the entire series. Furthermore, the values of ΔMSDA for the M–O(1) and M–O(2) bonds increase with increasing mole fraction of chromium through the solid solutions, while for M–O(3) the value of ΔMSDA remains essentially constant with a magnitude in the range expected for a rigid covalent bond (Table 3). Fig. 12 shows the M–O(1) bond with the thermal ellipsoids of its terminal atoms for the entire series of solutions, and the progressive enlargement of the O(1) site with increasing x(Cr) is easily observed. (The utility of displacement ellipsoid montages in examining disordered Jahn–Teller systems had previously been demonstrated by Simmons *et al.*[33] and by Hathaway,[14] among others.)

A simple interpretation that is consistent with all of the data observed at room temperature is that the formation of solid solutions effects a fuller level of disorder at the chromium center, and that both M–O(1) and M–O(2) occupy their near and distant positions with roughly equal populations. The chromium complex has four short and two long Cr–O bonds, with the two long bonds *trans* to each other. In the solid solutions a tetragonal elongation is disordered over two sets of Cr–O bonds, giving average, apparent bond lengths for both M–O(1) and M–O(2). Being averages of long and short Cr–O distances superposed on Zn–O distances, the apparent bond lengths for M–O(1) and M–O(2) appear to be longer than the short distance M–O(3) and thus give the deceptive appearance of a system with one short and two long pairs of M–L bonds. Since the observed distances for M–O(1) and M–O(2) are averages of three distinct entities, namely Zn–O, Cr–O (short), and Cr–O (long), and are weighted by the population of each in the crystal, the observed distances decrease with decreasing values of x(Cr). The question of whether the disorder is static or dynamic remains open, and could in principle be resolved by diffraction studies at several temperatures, or by EPR measurements. A final point of importance is that in the solid solutions it is M–O(1) that is slightly longer than M–O(2), whereas in the pure chromium complex the Jahn–Teller elongation rests principally with M–O(2).

Further light was shed on the behavior of the Cr/Zn Tutton salt solid solutions by single-crystal neutron diffraction analyses at temperatures of 11–16 K of two relatively low-x(Cr) (0.10 and 0.22) samples.[50] In that study it was found by examination of anisotropic displacement parameters that much or all of the disorder between Cr- and Zn-containing sites at very low temperature was localized in the M–O(1) direction. Since the concentration of chromium was low, the apparent bond lengths showed significant but still only slight differences indicating the direction of the JT distortion at the chromium center. However, the ΔMSDA values gave a clearer indication: for the sample with x(Cr) = 0.22 and using units of 10^{-4} Å^2 the ΔMSDA values were 127, 11 and 15 for M–O(1), M–O(2) and M–O(3), respectively; for x(Cr) = 0.10, the corresponding values were 70, 13 and 14. It was possible, moreover, to estimate the difference between the Cr–O(1) and Zn–O(1) bond lengths at the disordered site, using the ΔMSDA values and a formula derived by Stebler and Bürgi.[41] The results, Δd[M–O(1)] = 0.26 Å for x(Cr) = 0.22 and Δd[M–O(1)] = 0.25 Å for x(Cr) = 0.10 are both in rough accord with the difference of 0.213(2) Å between the relevant Cr–O and Zn–O distances derived from room-temperature X-ray analyses of the pure Cr- and Zn-containing Tutton salts.

Two major conclusions are evident from the structural results on the mixed Cr/Zn Tutton salts. First, the appearance of Jahn–Teller compression in the bond distances is in this case a structural chimera, and arises because of disorder. This phenomenon has been studied in great depth in recent years by Hitchman, Reinen and co-workers,[51–53] who have used X-ray diffraction, EXAFS, and EPR measurements to expose the tetragonally elongated nature of a series of copper complexes that under routine diffraction analysis appear to possess Jahn–Teller compression. An early study by Friebel and Reinen[54] demonstrated the manner in which an elongated Jahn–Teller complex could appear to be compressed. To this author's knowledge, there is presently just one verified example of a homoleptic six-co-ordinate Jahn–Teller complex with an oblate shape in an undoped phase, namely $[CuF_6]^{4-}$ in $KAlCuF_6$.[55] All presently available evidence indicates that the chromium complexes in the Tutton salt solid solutions are distorted by elongation.

The second important feature of the results from the Tutton salts is that the Jahn–Teller distortion passes from being expressed principally as elongation of Cr–O(2) in the pure salt at room temperature, to being disordered between the Cr–O(1) and Cr–O(2) directions in all of the solid solutions at room temperature, but with Cr–O(1) favored, to being an elongation along Cr–O(1) at the very low temperatures (11–16 K) of the neutron diffraction analyses of the low-x(Cr) solutions. In terms of the adiabatic potential energy surface of Fig. 3, these results correspond to a shift from population of one energy minimum for the pure chromium system at room temperature to simultaneous population of the first and a second minimum in the solid solutions at room temperature, proceeding to population only of the second minimum in the dilute solutions at very low temperature. It should be stressed that the potential energy surface does not maintain the idealized shape of the schematic in Fig. 3, but rather is further warped by the perturbations of solid-solution formation and temperature change. Accompanying the molecular shape change of the Jahn–Teller complex is a single modification of the hydrogen-bonding pattern in the extended structure and a concomitant slight tilt of the sulfate group. Thus, a crystal with elongation of Cr–O(1) is not formally isomorphous with one in which Cr–O(2) is elongated. The structural change observed here is closely related to the Jahn–Teller switch to be described presently.

While primary attention has been focused here on the structural aspects of the molecular solid solution studies, the synthetic work in this area also requires special attention. It is particularly important to avoid the formation of concentration gradients in the single-crystal samples. The presence of significant inhomogeneity in a crystal would render invalid any results derived through single-crystal diffraction, for the experiment would then average the concentration-dependent results over the entire sample. Such an occurrence would not go unnoticed, fortunately, as the small but significant differences in cell dimensions and in experimental observables such as diffraction spot shape as a function of x(Cr) make it possible to identify inhomogeneous samples. The preparations of the mixed crystals were adapted to the purpose of producing homogeneous samples. The main features of the preparative procedures were the use of relatively large quantities of liquid reaction mixtures and the early harvesting of the first few crystals that appeared and no others. By this means the large majority of crystals that were examined were judged homogeneous. Detailed descriptions of the preparative procedures are given in the publications on the molecular solid solutions.[40,44,49]

A final point on the molecular solid solutions involves the determination of x(Cr) for the solid samples. In the three studies described here the relative molar populations of chromium and zinc were determined from the diffraction data, and thorough discussions of the validity of this procedure were given for the studies on the saccharinates[40] and nicotinates.[44] It was shown that the population parameter a in the composite scattering factor $[a{\cdot}f(\mathrm{Cr}) + (1 - a){\cdot}f(\mathrm{Zn})]$ [f(Cr) and f(Zn) are the scattering factors of the respective elements] has approximately as much significance in the least-squares refinements as does a positional parameter for a light atom such as carbon. The reliability of the populations thus determined was tested in the study of the Tutton salts, for which atomic absorption analysis was also used to determine the concentrations of several of the samples. The results from the two methods agreed to within experimental error.

The Jahn–Teller Switch

It has been known for some time that the Tutton salts of copper, $A_2[Cu(H_2O)_6][SO_4]_2$, in which A is a monocation, display an unusual structural behavior dependent on the nature of A. Although the structures of all of the salts are similar, nearly isotypic, the direction of the Jahn–Teller elongation rests with one set of *trans*-Cu–O bonds in some of the salts, *i.e.* for A = K^+, Rb^+ and Cs^+,[14] while it shifts to another set of Cu–O bonds, perpendicular to the first, in the NH_4^+ salt.[48,56] Furthermore, the deuteriated ammonium salt, $[ND_4]_2[Cu(D_2O)_6][SO_4]_2$, does not have the same distortion as its hydrogenated analogue, but rather has that of the K^+, Rb^+ and Cs^+ salts.[57] As described above, moreover, the ammonium chromium Tutton salt undergoes a distortion shift upon being doped into the zinc analogue, with the shift passing from the form of dynamic behavior in the solid solutions at room temperature to a full shift at near-liquid-helium temperature. These observations indicate the presence of two favorable, closely related structure types involving two distinct molecular distortions of the Jahn–Teller-active cations.

A key extension of these observations was reported recently, in which the deuteriated ammonium copper Tutton salt was made to switch in real time from one distortion to another.[58] This 'Jahn–Teller switch' was brought on by the application of pressure. As described for the Cr/Zn solid solutions, a potential energy surface such as that of Fig. 3 is a useful aide in the interpretation of the Jahn–Teller switch; in this case the surface must be modified to account for structure- and pressure-induced strain. The Jahn–Teller system passes from one potential energy well corresponding to one tetragonally elongated structure at 15 K and 1 bar (10^5 Pa) pressure to another energy minimum corresponding to another tetragonal elongation at 15 K and 1.5 kbar pressure. These results were further refined by

the recent characterization of the reversibility (with hysteresis) of the transformation.[59] In addition, a thorough characterization has also been reported of the structural response of the deuteriated ammonium copper Tutton salt to increased pressure at room temperature, where the Jahn–Teller ion exhibits a certain degree of two-dimensional fluxionality.[60] Nevertheless, the same 'switch' from principal elongation of one set of bonds at low pressure to elongation of another set at higher pressures is observed.

The earlier observation that the ammonium copper Tutton salt exhibits a structural isotope effect in which the Jahn–Teller elongation occurs along one set of Cu–O bonds in $[NH_4]_2[Cu(H_2O)_6][SO_4]_2$ and along another in $[ND_4]_2[Cu(D_2O)_6][SO_4]_2$ was an interesting result in itself. However, the real-time, reversible switch from one tetragonal distortion to another in the deuteriated salt is an opening to an entirely different line of investigation, especially as it comes at a time of rapidly growing interest in molecular devices, molecules that change shape, undergo shifts in the directions of anisotropic properties, or exhibit some other measurable and thus potentially exploitable change in response to an external stimulus.

Conclusion

The theorem of Jahn and Teller gives a fundamental explanation for a variety of superficially disparate phenomena that have a common origin in symmetry-lowering vibronic interactions. In their simplest and commonest expression, that of static tetragonal distortion of octahedral d^9 or high-spin d^4 complexes, Jahn–Teller effects form a staple of co-ordination chemistry. The use of adiabatic potential energy surfaces in explaining such simple manifestations of Jahn–Teller behavior offers a conceptual link to clear explanations of more complex phenomena, dynamic Jahn–Teller systems, Jahn–Teller-active compounds in undistorted host lattices, or the recently discovered Jahn–Teller switch, to name a few.

The study of Jahn–Teller phenomena, as a research topic, has been notably resistant to scientific senescence. Through the six decades since the theorem was put forward, advances in the understanding of Jahn–Teller effects have accompanied advances in such varied areas of study as copper chemistry, thermal-motion and displacement analysis from diffraction, and spectroscopy. Recent advances in the practical understanding of Jahn–Teller effects in the solid state, and particularly in the use of adiabatic potential energy surfaces for explaining new systems, should serve as a useful foundation for future studies. Results such as the observation of the Jahn–Teller switch and the implication of Jahn–Teller centers in phenomena such as colossal magnetoresistance suggest that Jahn–Teller effects still present much scope for further work in areas of potentially wide applicability.

Acknowledgements

The author thanks the Dirección General de Enseñanza Superior (Spain) for financial support through Grant PB95-0792.

References

1 R. Englman, B. Halperin and M. Weger, *Physica C*, 1990, **169**, 314.
2 Yu. B. Gaididei and V. M. Loktev, *Phys. Status Solidi*, 1988, **147**, 307.
3 W. Weber, A. L. Shelankov and X. Zotos, *Physica C*, 1989, **162–164**, 307.
4 D. V. Fil, O. I. Tokar, A. L. Shelankov and W. Weber, *Phys. Rev. B*, 1992, **45**, 5633.
5 S. Jin, T. H. Tiefel, M. McCormack, R. A. Fastnacht, R. Ramesh and L. H. Chen, *Science*, 1994, **264**, 413.
6 A. J. Millis, P. B. Littlewood and B. I. Shraiman, *Phys. Rev. Lett.*, 1995, **74**, 5144.
7 A. P. Ramirez, P. Schiffer, S.-W. Cheong, C. H. Chen, W. Bao, T. T. M. Palstra, P. L. Gammel, D. J. Bishop and B. Zegarski, *Phys. Rev. Lett.*, 1996, **76**, 3188.
8 H. A. Jahn and E. Teller, *Proc. R. Soc. London*, *Ser. A*, 1937, **161**, 220.
9 H. A. Jahn, *Proc. R. Soc. London*, *Ser. A*, 1938, **164**, 117.
10 W. L. Clinton and B. Rice, *J. Chem. Phys.*, 1959, **30**, 542.
11 C. J. Simmons, *New J. Chem.*, 1993, **17**, 77.
12 B. Hathaway, M. Duggan, A. Murphy, J. Mullane, C. Power, A. Walsh and B. Walsh, *Coord. Chem. Rev.*, 1981, **36**, 267.
13 B. Hathaway, *Coord. Chem. Rev.*, 1981, **35**, 211.
14 B. J. Hathaway, *Struct. Bonding (Berlin)*, 1984, **57**, 56.
15 I. B. Bersuker, *Coord. Chem. Rev.*, 1975, **14**, 357.
16 M. A. Hitchman, *Comments Inorg. Chem.*, 1994, **15**, 197.
17 I. B. Bersuker, *Stroenie i svoistva coordinationich soedinenii. Vuedenie u teoriu* (Structure and Properties of Coordination Compounds. Introduction to the Theory), Chimia, Leningrad, 1971; cited in ref. 15.
18 H. C. Longuet-Higgins, *Adv. Spectrosc.*, New York, 1961, **2**, 429; cited in ref. 15.
19 J. H. Ammeter, H. B. Bürgi, E. Gamp, V. Meyer-Sandrin and W. P. Jensen, *Inorg. Chem.*, 1979, **18**, 733.
20 L. E. Orgel and J. D. Dunitz, *Nature (London)*, 1957, **179**, 462.
21 J. D. Dunitz and L. E. Orgel, *J. Phys. Chem. Solids*, 1957, **3**, 20.
22 B. Bleaney and D. J. E. Ingram, *Proc. Phys. Soc. London*, *Ser. A*, 1950, **63**, 408.
23 A. Abragam and M. H. L. Pryce, *Proc. Phys. Soc. London*, *Ser. A*, 1950, **63**, 409.
24 B. Bleaney and K. D. Bowers, *Proc. Phys. Soc. London*, *Ser. A*, 1952, **65**, 667.
25 D. Reinen and M. Atanasov, *Magn. Reson. Rev.*, 1991, **15**, 167.
26 M. J. Riley, M. A. Hitchman and D. Reinen, *Chem. Phys.*, 1986, **102**, 11.
27 M. J. Riley, M. A. Hitchman and A. Wan Mohammed, *J. Chem. Phys.*, 1987, **87**, 3766.
28 M. J. Riley, M. A. Hitchman, D. Reinen and G. Steffen, *Inorg. Chem.*, 1988, **27**, 1924.
29 A. C. Blackburn, J. C. Gallucci and R. E. Gerkin, *Acta Crystallogr.*, *Sect. C*, 1991, **47**, 2019.
30 J. D. Dunitz, V. Schomaker and K. N. Trueblood, *J. Chem. Phys.*, 1988, **92**, 856; THMA 11, K. N. Trueblood, personal communication.
31 F. A. Cotton, L. R. Falvello, C. A. Murillo and J. F. Quesada, *J. Solid State Chem.*, 1992, **96**, 192.
32 D. Mullen, G. Heger and D. Reinen, *Solid State Commun.*, 1975, **17**, 1249.
33 C. J. Simmons, B. J. Hathaway, K. Amornjarusiri, B. D. Santarsiero and A. Clearfield, *J. Am. Chem. Soc.*, 1987, **109**, 1947.
34 C. J. Simmons, A. Clearfield, W. Fitzgerald, S. Tyagi and B. J. Hathaway, *Inorg. Chem.*, 1983, **22**, 2463.
35 C. Simmons, A. Clearfield, W. Fitzgerald, S. Tyagi and B. Hathaway, *J. Chem. Soc.*, *Chem. Commun.*, 1983, 189.
36 C. J. Simmons, A. Clearfield, W. Fitzgerald, S. Tyagi and B. J. Hathaway, *Trans. Am. Crystallogr. Assoc.*, 1984, **20**, 155.
37 F. A. Cotton, G. E. Lewis, C. A. Murillo, W. Schwotzer and G. Valle, *Inorg. Chem.*, 1984, **23**, 4038.
38 K. J. Ahmed, A. Habib, S. Z. Haider, K. M. A. Malik and M. B. Hursthouse, *Inorg. Chim. Acta*, 1981, **56**, L37; S. Z. Haider, K. M. A. Malik, K. J. Ahmed, H. Hess, H. Riffel and M. B. Hursthouse, *Inorg. Chim. Acta*, 1983, **72**, 21.
39 F. A. Cotton, L. R. Falvello, C. A. Murillo and A. J. Schultz, *Eur. J. Solid State Inorg. Chem.*, 1992, **29**, 311.
40 F. A. Cotton, L. R. Falvello, C. A. Murillo and G. Valle, *Z. Anorg. Allg. Chem.*, 1986, **540/541**, 67.
41 M. Stebler and H. B. Bürgi, *J. Am. Chem. Soc.*, 1987, **109**, 1395.
42 W. E. Broderick, M. R. Pressprich, U. Geiser, R. D. Willett and J. I. Legg, *Inorg. Chem.*, 1986, **25**, 3372.
43 J. A. Cooper, B. F. Anderson, P. D. Buckley and L. F. Blackwell, *Inorg. Chim. Acta*, 1984, **91**, 1.
44 F. A. Cotton, L. R. Falvello, E. L. Ohlhausen, C. A. Murillo and J. F. Quesada, *Z. Anorg. Allg. Chem.*, 1991, **598/599**, 53.
45 E. N. Maslen, K. J. Watson and F. H. Moore, *Acta Crystallogr.*, *Sect. B*, 1988, **44**, 102; B. N. Figgis, E. S. Kucharski and P. A. Reynolds, *Acta Crystallogr.*, *Sect. B*, 1990, **46**, 577; B. N. Figgis, L. Khor, E. S. Kucharski and P. A. Reynolds, *Acta Crystallogr.*, *Sect. B*, 1992, **48**, 144; B. N. Figgis, C. J. Kepert, E. S. Kucharski and P. A. Reynolds, *Acta Crystallogr.*, *Sect. B*, 1992, **48**, 753; B. N. Figgis, B. B. Iversen, F. K. Larsen and P. A. Reynolds, *Acta Crystallogr.*, *Sect. B*, 1993, **49**, 794.
46 B. B. Iversen, F. K. Larsen, P. A. Reynolds and B. N. Figgis, *Acta Chem. Scand.*, 1994, **48**, 800.
47 G. S. Chandler, G. A. Christos, B. N. Figgis and P. A. Reynolds, *J. Chem. Soc.*, *Faraday Trans.*, 1992, 1961.

48 N. W. Alcock, M. Duggan, A. Murray, S. Tyagi, B. J. Hathaway and A. Hewat, *J. Chem. Soc.*, *Dalton Trans.*, 1984, 7.
49 M. A. Araya, F. A. Cotton, L. M. Daniels, L. R. Falvello and C. A. Murillo, *Inorg. Chem.*, 1993, **32**, 4853.
50 F. A. Cotton, L. M. Daniels, L. R. Falvello, C. A. Murillo and A. J. Schultz, *Inorg. Chem.*, 1994, **33**, 5396.
51 T. Astley, H. Headlam, M. A. Hitchman, F. R. Keene, J. Pilbrow, H. Stratemeier, E. R. T. Tiekink and Y. C. Zhong, *J. Chem. Soc.*, *Dalton Trans.*, 1995, 3809.
52 P. J. Ellis, H. C. Freeman, M. A. Hitchman, D. Reinen and B. Wagner, *Inorg. Chem.*, 1994, **33**, 1249.
53 H. Stratemeier, B. Wagner, E. R. Krausz, R. Linder, H.-H. Schmidtke, J. Pebler, W. E. Hatfield, L. ter Haar, D. Reinen and M. A. Hitchman, *Inorg. Chem.*, 1994, **33**, 2320.
54 C. Friebel and D. Reinen, *Z. Anorg. Allg. Chem.*, 1974, **407**, 193.
55 M. Atanasov, M. A. Hitchman, R. Hoppe, K. S. Murray, B. Moubaraki, D. Reinen and H. Stratemeier, *Inorg. Chem.*, 1993, **32**, 3397; K. Finnie, L. Dubicki, E. R. Krausz and M. J. Riley, *Inorg. Chem.*, 1990, **29**, 3908; G. Wingefeld and R. Hoppe, *Z. Anorg. Allg. Chem.*, 1984, **516**, 223.
56 H. Montgomery and E. Lingafelter, *Acta Crystallogr.*, 1966, **20**, 659; G. M. Brown and R. Chidambaram, *Acta Crystallogr.*, *Sect. B*, 1969, **25**, 676,.
57 B. J. Hathaway and A. W. Hewat, *J. Solid State Chem.*, 1984, **51**, 364.
58 C. J. Simmons, M. A. Hitchman, H. Stratemeier and A. J. Schultz, *J. Am. Chem. Soc.*, 1993, **115**, 11 304.
59 A. J. Schultz, M. A. Hitchman, J. D. Jorgensen, S. Lukin, P. G. Radaelli, C. J. Simmons and H. Stratemeier, *Inorg. Chem.*, 1997, **36**, 3382.
60 W. Rauw, H. Ahsbahs, M. A. Hitchman, S. Lukin, D. Reinen, A. J. Schultz, C. J. Simmons and H. Stratemeier, *Inorg. Chem.*, 1996, **35**, 1902.

Received 22*nd May* 1997; *Paper* 7/03548I